BASIC SCIENCE

Nanomedicine: Nanotechnology, Biology, and Medicine
17 (2019) 198 – 209

Original Article

nanomedjournal.com

Poly(propylene imine) dendrimers with histidine-maltose shell as novel type of nanoparticles for synapse and memory protection

Ester Aso, PhD[a,e], Isak Martinsson, MSc[b], Dietmar Appelhans, PhD[c], Christiane Effenberg, MSc[c], Nuria Benseny-Cases, PhD[d,e], Josep Cladera, PhD[d], Gunnar Gouras, MD, PhD[b], Isidre Ferrer, MD, PhD[a,f], Oxana Klementieva, PhD[a,b,*]

[a]*Institute of Neuropathology, IDIBELL-University Hospital Bellvitge, L'Hospitalet de Llobregat, Spain*
[b]*Wallenberg Neuroscience Center, Lund University, Lund, Sweden*
[c]*Leibniz Institute of Polymer Research Dresden, Dresden, Germany*
[d]*Universitat Autònoma de Barcelona, Bellaterra, Spain*
[e]*ALBA Synchrotron Light Source, Cerdanyola del Vallès, Spain*
[f]*CIBERNED, Instituto Carlos III, Spain*

Revised 17 December 2018

Abstract

Poly(propylene imine) dendrimers have been shown to be promising 3-dimensional polymers for the use in the pharmaceutical and biomedical applications. Our aims of this study were first, to synthesize a novel type of dendrimer with poly(propylene imine) core and maltose-histidine shell (G4HisMal) assessing if maltose-histidine shell can improve the biocompatibility and the ability to cross the blood-brain barrier, and second, to investigate the potential of G4HisMal to protect Alzheimer disease transgenic mice from memory impairment. Our data demonstrate that G4HisMal has significantly improved biocompatibility and ability to cross the blood-brain barrier in vivo. Therefore, we suggest that a maltose-histidine shell can be used to improve biocompatibility and ability to cross the blood-brain barrier of dendrimers. Moreover, G4HisMal demonstrated properties for synapse and memory protection when administered to Alzheimer disease transgenic mice. Therefore, G4HisMal can be considered as a promising drug candidate to prevent Alzheimer disease via synapse protection.

Key words: Dendrimers; Histidine; Maltose; Biocompatibility; Amyloid; Synapses

Alzheimer's disease (AD) is an age-dependent neurodegenerative process characterized by the presence of senile plaques mainly composed of different species of aggregated β-amyloid (Aβ), and by the presence of neurofibrillary tangles, mostly composed of various isoforms of hyperphosphorylated tau protein.[1] At present, there is no effective treatment, which could stop or delay AD progression. It is already accepted that loss of synapses is considered the best pathological correlate of cognitive decline[2–4] and the link between soluble Aβ aggregates (oligomers) and synapse degradation is already established.[5,6] Thus, one direction for AD therapies could be protection of synapses, which includes finding molecules that can protect

Abbreviations: AD, Alzheimer disease; BBB, Blood-brain barrier; G3Mal, Maltose modified PPI dendrimers of 3rd generation; G4HisMal, Maltose modified PPI dendrimers of 3rd generation; FITC, Fluorescein-5/6-isothiocyanate; LDH, Cytotoxicity assay based on colorimetric measurements of lactate dehydrogenase activity; MTT, Cell proliferation assay based on colorimetric measurements of tetrazolium dye 3- (4,5-dimethylthiazol-2-yl)-2,5-diphenyltetrazolium bromide; PAMAM, Polyamidoamine; PEG, Polyethyleneglycol; PPI, Poly(propylene imine); ThT, Thioflavin T; ThS, Thioflavin S; SAXS, Small angle x-ray scattering; MALDI-TOF, Matrix Assisted Laser Desorption/Ionization Time of Flight Mass Spectrometry

Conflict of Interests: There is no financial or personal interest or belief that could affect authors' objectivity or could be the source and nature of a potential conflict.

*Corresponding author at: Wallenberg Neuroscience Center, Lund University, BMC B10, Sölvegatan 19, 22184 Lund, Sweden.
E-mail address: oxana.klementieva@med.lu.se (O. Klementieva).

https://doi.org/10.1016/j.nano.2019.01.010

Please cite this article as: Aso E, et al, Poly(propylene imine) dendrimers with histidine-maltose shell as novel type of nanoparticles for synapse and memory protection. *Nanomedicine: NBM* 2019;17:198-209, https://doi.org/10.1016/j.nano.2019.01.010

synapses against the damage associated with soluble Aβ oligomers.

In this study, we used 3-dimensionally branched macromolecules called dendrimers. Dendrimers are built by a series of iterative synthetic steps from a small core molecule, propylene imine in our case. Dendrimers have important features such as controlled structure, nanoscopic size and high tunable availability of multiple functional groups at their surface.[7] In medical applications, dendrimers have high potential as drug nanocarriers, imaging agents or as drugs per se.[8] However, the ability to cross the blood−brain-barrier (BBB) has been shown only for few types of dendrimers, such as polyamidoamine (PAMAM) dendrimer–drug conjugates,[9–11] and maltose poly(propylene imine) dendrimers.[12] Previously we have reported that maltose shell significantly reduces poly(propylene imine) (PPI) dendrimers of 3rd generation toxicity (G3Mal) in vivo and allows G3Mal to cross blood−brain-barrier. However, in spite of confirmed anti-amyloidogenic properties, G3Mal has not been able to improve memory deficits in APP/PS1 transgenic mice.[12]

For the present study, we synthesized a novel type of dendrimers: poly(propylene imine) dendrimers with a histidine-maltose shell (G4HisMal). Histidine was selected due to several reasons: is selectively transported through the BBB[13] it has chelating properties for Cu^{2+} ions[14] which is considered to be important since metal ion dyshomeostasis plays a detrimental role in oxidative stress related to AD progression[15]; it has some neuroprotective capacity.[16] For dendrimers modification, histidine was combined with maltose, since G3Mal has been proved as non-toxic antiamyloidogenic agents capable to cross BBB.[12] Here, we hypothesized that due to maltose PPI dendrimers may keep anti-amyloidogenic properties meanwhile the added histidine may help PPI dendrimer to cross BBB and will add neuroprotective properties.

Using in vitro and in vivo models of AD, we characterized the anti-amyloidogenic and neuroprotective properties G4HisMal. Here we report that G4HisMal had significantly improved biocompatibility and the ability of cross BBB. We proved that G4HisMal crossed BBB, and did not accumulate in the brain tissue being well-tolerated since treated no visible signs of weaknesses or apathy in mouse behavior were recorded during all period of chronic treatment. Strikingly, G4HisMal treatment prevented memory decline during AD-like pathology. Our data demonstrated that the positive cognitive effects induced by G4HisMal in aged AD transgenic mice were not associated with insoluble Aβ load reduction but with synapse protection.

Methods

Reagents

PPI dendrimer of the 5th generation with 64 terminal amino groups and 4th generation with 32 terminal amino groups was obtained from SyMO-Chem (Eindhoven, The Netherlands) and specified as 4th generation PPI dendrimers (PPI G4) and 3rd PPI dendrimer (PPI G3) following the uniform nomenclature description of polyamine dendrimers,[17] this nomenclature was also applied for other previously published PPI dendrimers and cited in the present text (ref. 12, 35 and 36).

Maltose monohydrate, L-histidine, sodium borate, boran pyridine complex, and fluorescein-5/6-isothiocyanate (FITC) were purchased from Sigma-Aldrich (Germany).

$A\beta_{(1-40)}$, with the amino acid sequence: [DAEFRHDSGYEVHHQKLVFFAEDVGSNKGAIIG LMVGGVV], was obtained from JPT Peptide Technologies GmbH (Germany).

$A\beta_{(1-42)}$, with the amino acid sequence: [DAEFRHDSGYEVHHQKLVFFAEDVGSNKGAIIG LMVGGVVIA], was obtained from Tocris (USA). Amyloid peptides were dissolved in 10 mmol HEPES buffer (Sigma-Aldrich Spain, Sweden) with 0.02 % NH_3 at pH 12; stock concentration was 250 μmol; aliquots were kept at −80°C until use.

Synthesis of G4HisMal dendrimer

Synthesis of G4HisMal was performed in two steps: First, Poly(propylene imine) dendrimers of the 4th generation were modified with His (G4His), then G4His was modified with maltose (G4HisMal).

The whole conversion process was carried out under argon protection atmosphere. G4 dendrimer (0.135 g (1 equivalent); 1.88×10^{-5} mol) was freeze-dried overnight, while anhydrous DMSO (5 mL) was additionally pretreated under stirring in high vacuum condition for several hours to dissolve freeze-dried G4 dendrimer and triethylamine (0.142 mL). A second reaction solution was prepared to unify *N*-Boc-L-histidine (125 mg; 26 equivalents; 4.9×10^{-4} mol) and BOP (283 mg; 34 equivalents related to *N*-Boc-L-histidine; 6.4×10^{-4} mol) in 10 mL anhydrous DMSO and, then, stirred for 1 hour at room temperature. The ester-activated *N*-Boc-L-histidine solution was slowly added to the dendrimer solution. Then, the corresponding reaction mixture was stirred for 24 hours at room temperature. The reaction solution was intensively dialyzed in bidistilled water for 3 days using dialysis tube with 1000 MWCO (ZelluTrans, Roth (Germany), Flat with 45 mm) by exchanging bidistilled water at least 3 times per day (5l beaker glass). To obtain solid material for G4His with 99% yield 2-step freeze-drying was done by reconstitution of the dialyzed product in 5 mL bidistilled water for the second freeze-drying process. G4His was characterized by ^{1}H and ^{13}C NMR and mass spectrometry (Supplementary Figures 1-3).

G4His (0.1 g (1 equivalent); 7.5 × 10-6 M), D(+)-maltose monohydrate (5.513 g (nearly 32 equivalents for each amino group of G4His), 15.3 mmol), and borane-pyridine complex (3.4 mL; 15.3 mmol; 8 mol solution) were taken up in a sodium borate buffer (15 mL; 0.1 mol). The reaction solution was stirred at 50°C for 7 days. Then, the crude product was purified by dialysis towards bidistilled water for 3 days, exchanging water at least three times per day. G4HisMal was obtained from freeze-drying process. The yield was (0.95 g, 72 %). Conversion of the G4HisMal with FITC was used for the detection and mapping of G4HisMal in cells and brain tissue. Synthesis of FITC-labeled dendrimers was done as described.[18] Synthetic pathways for G4HisMal is presented in Figure 1. Description of characterization of dendrimers is described in Supplementary Information.

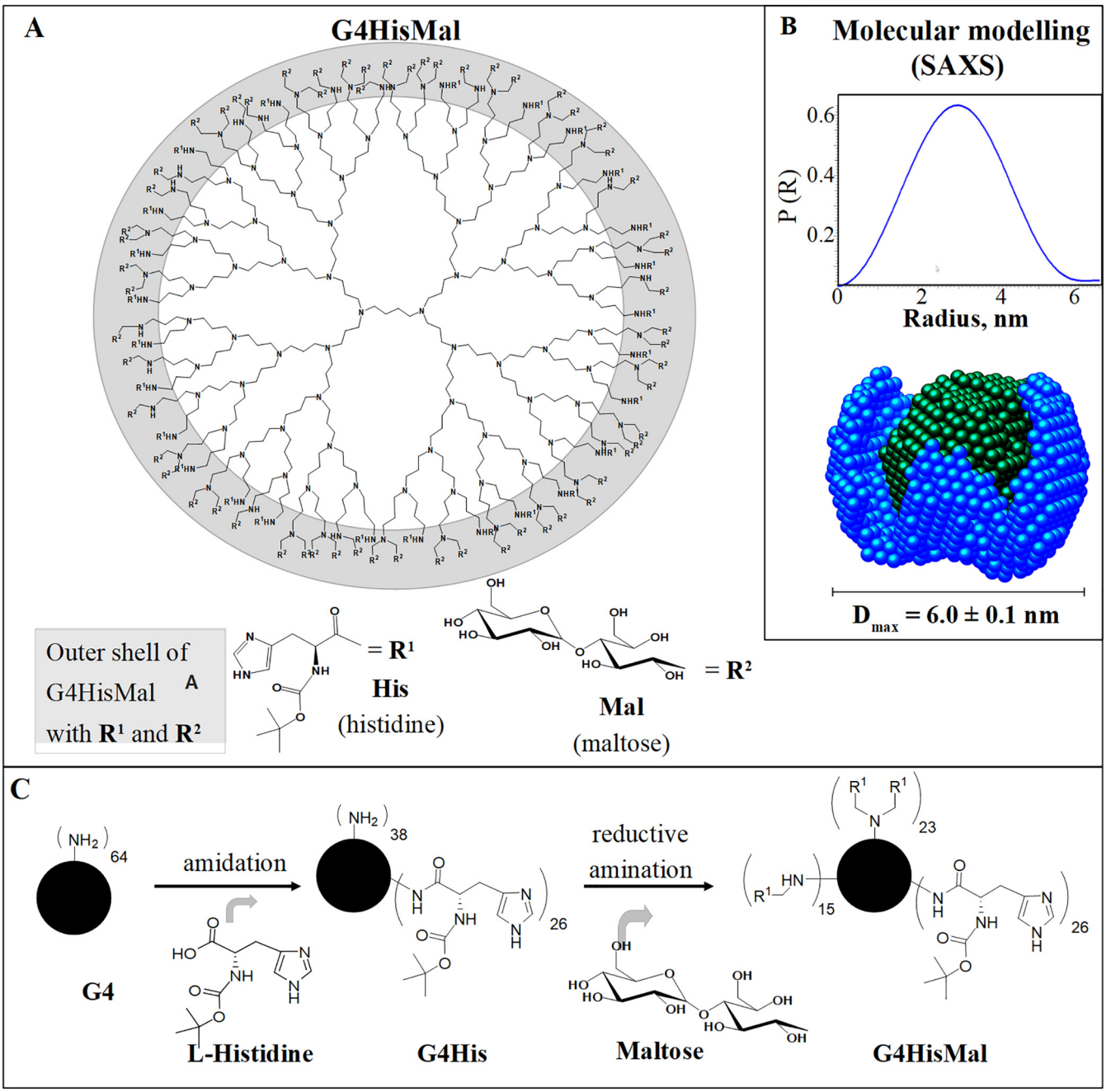

Figure 1. Structure and synthesis of G4HisMal. (**A**) Simplified structure of G4HisMal. Layers 1-4 indicate dendrimer's branching points and generation of the dendrimer. Layer 4 shows N terminal groups with maltose as R1 and histidine as R2 substituents. (**B**) Distance distribution functions P(R) of G4HisMal in PBS calculated SAXS pattern of G4HisMal in PBS at 37°C using GNOM.[40] Insertion: De novo three-dimensional reconstruction of the scattering entity of G4HisMal using DAMMIF after 10 independent reconstructions. A line indicates the maximum dimension (Dmax), UCSF Chimera[41] was used for visualization. The SAXS raw data model fitting is shown in Supplementary Figure 7. (**C**) Reaction pathway for synthesizing glycodendrimer G4HisMal.

Design of experiments in vivo

The experiments carried out on male APP/PS1 and wild-type mice. Two experimental treatment settings were designed, covering short-term intranasal administration (BBB cross), and long-term intranasal administration (treatment).

BBB cross

Short-term intranasal administration was conducted in non-transgenic littermates aged 6 months treated with FITC −G4HisMal, or the PBS (n = 3 per group) by applying two equal drops with a micropipet to each nasal cavity (5 μL), resulting in a total dose of 10 mg/kg/body weight. After 1 hour,

the animals were perfused through the left cardiac ventricle with cold PBS pH 7.4 under deep whole-body anesthesia (ketamine/xylazine, 5:1; 0.10 mL/10g/body weight, intraperitoneally). When blood was cleaned up from the brain blood vessels, the brains were removed, one brain hemisphere was homogenized, while the second one was snap frozen and stored at −80°C until use.

G4HIsMal treatment

At the age of 3 months animals were randomly divided as follows: 7 transgenic and 6 WT mice received 5 μg per day G4HisMal; 5 transgenic and 6 WT mice received the same volume of PBS (5 μL). Long-term intranasal administration lasted 3 months until animals reached of age of 6 months.

Memory evaluation tests were performed at the end of long-term intranasal treatment using two object recognition test in a V-maze (Panlab, Barcelona, Spain) as described.[19]

Fluorescent measurements of FITC-G4HisMal in mouse brain tissue extract

Frozen brain tissues were homogenized in 5 volumes (wt/vol) of TBS extraction buffer [140 mmol NaCl, 3 mmol KCl, 25 mmol Tris, pH 7.4, 5 mmol EDTA, and protease inhibitor cocktail (Roche, Madrid, Spain)]. Homogenates were spun at 100000 g for 1 hour, and the supernatants were saved as the brain soluble fractions. Quantitative determination of $A\beta_{(1-40)}$ and $A\beta_{(1-42)}$ in brain soluble fractions was carried out using $A\beta_{(1-40)}$ and $A\beta_{(1-42)}$ human ELISA kits (Invitrogen, U.S.A.) according to the instructions of the manufacturer.

Fluorescent measurements were performed immediately after preparation of tissue extracts, the fluorescence of FITC labeled dendrimers was recorded at 485 nm excitation and 500−700 nm emission wavelength as described.[18] The background was set as an intrinsic fluorescence of brain homogenate treated with PBS. The content of FITC-labeled dendrimers was quantified with standard curves of FITC-labeled dendrimers and expressed per gram of tissue.

Double-labeling immunofluorescence and imaging

Brain tissue sections were immnolabeled as described[19] with combinations of primary antibodies (Supplementary Table 1) according to manufacturer protocols. For Thioflavin S (Th S) staining, sections were incubated with 1 % ThS (Sigma) in 70 % ethanol for 10 minutes. For imaging, we used confocal microscopes Leica TCS SP8 or Leica TCS (Leica Microsystems) equipped with Diode 405/405 nm and Argon (405, 488, 552, 638 nm) lasers with an HP PL APO 63x/NA1.2 water immersion objectives.

Immunofluorescence quantification

Amyloid burden was calculated as the percentage of the area of amyloid deposition in plaques with respect to the total cortical area. 9 pictures were taken from 3 different sections (-0.1 mm, -1.5 mm and -2.0 mm from bregma) of each animal brain. The pictures were taken from cingular/retrosplenial/motor cortex, somatosensory cortex and piriform/entorhinal cortex per each section. The areas selected were the main regions of the cerebral cortex in which Aβ is deposited in APP/PS1 mice. (n = 5, 6 per group).The Aβ burden was quantified using Adobe Photoshop CS4 software (Adobe Systems, San Jose, CA, USA) Specific immunolabeling densities (glial response, oxidative stress) were calculated in reference to the Aβ plaque area (6F/3D-positive) in 5 representative pictures taken from the cortex of each animal. Fibrillar amyloid burden was calculated as the percentage of the fibrillar (OC-positive) amyloid deposition area with respect to the total 6E10-positive area.

Cell culture

Human neuroblastoma cell line SH−SY5Y was purchased from the European Collection of Cell Cultures (ECACC) and were grown as described.[12] Primary neuronal cultures were generated from wild-type (wt) mouse embryos as described.[20]

Statistical analysis

Results of memory tests were analyzed with two-way ANOVA followed by Tukey's post hoc test. The data from the rest experiments tests were analyzed with one-way ANOVA followed by Tukey's post hoc test. In all the experiments, the significance level was set at $P < 0.05$.

Ethical issues

All in vivo experiments were approved by ethics committees of the Barcelona University (Principal Investigator: E. Aso) and Lund University (Principal Investigator: G. Gouras). In all experiments, we followed the guidelines of the Directive 2010/63/EU. Animals were housed in specific pathogen-free the Animal House of University of Barcelona and Lund University. The animals were maintained in 12 h light/dark cycles in a temperature regulated animal facility with free access to water and food.

Results

Maltose-histidine shell significantly improved the ability of poly (propylene imine) dendrimers to cross BBB

PPI dendrimers of 4th generation with primary surface amino groups were sequentially partially modified with histidine and maltose as described[21,22] (Figure 1, *A-C*). G4HisMal dendrimer structure was characterized by NMR spectroscopy; mass spectrometry; dynamic light scattering; synchrotron-based small angle x-ray scattering (SAXS) and MALDI-TOF mass spectroscopy: We determined the degree of substitution of histidine and maltose on the outer shell as 26 histidine and 61 maltose units, with resulting molecular mass of 34000 g/mol (Supplementary Figures 1–7). We used SAXS to study the overall shape and structure of G4HisMal in solution. SAXS data provided information on the shape and maximal diameter (6 nm) of G4HisMal. Interestingly that three-dimensional reconstruction of the scattering entity of G4HisMal revealed shell-like structure (Figure 1, *B*)

Since nanoparticles can pass rapidly from the nose into the brain along olfactory nerves, and the brain and brain stem along branches of the first and second trigeminal nerve structures,[23]

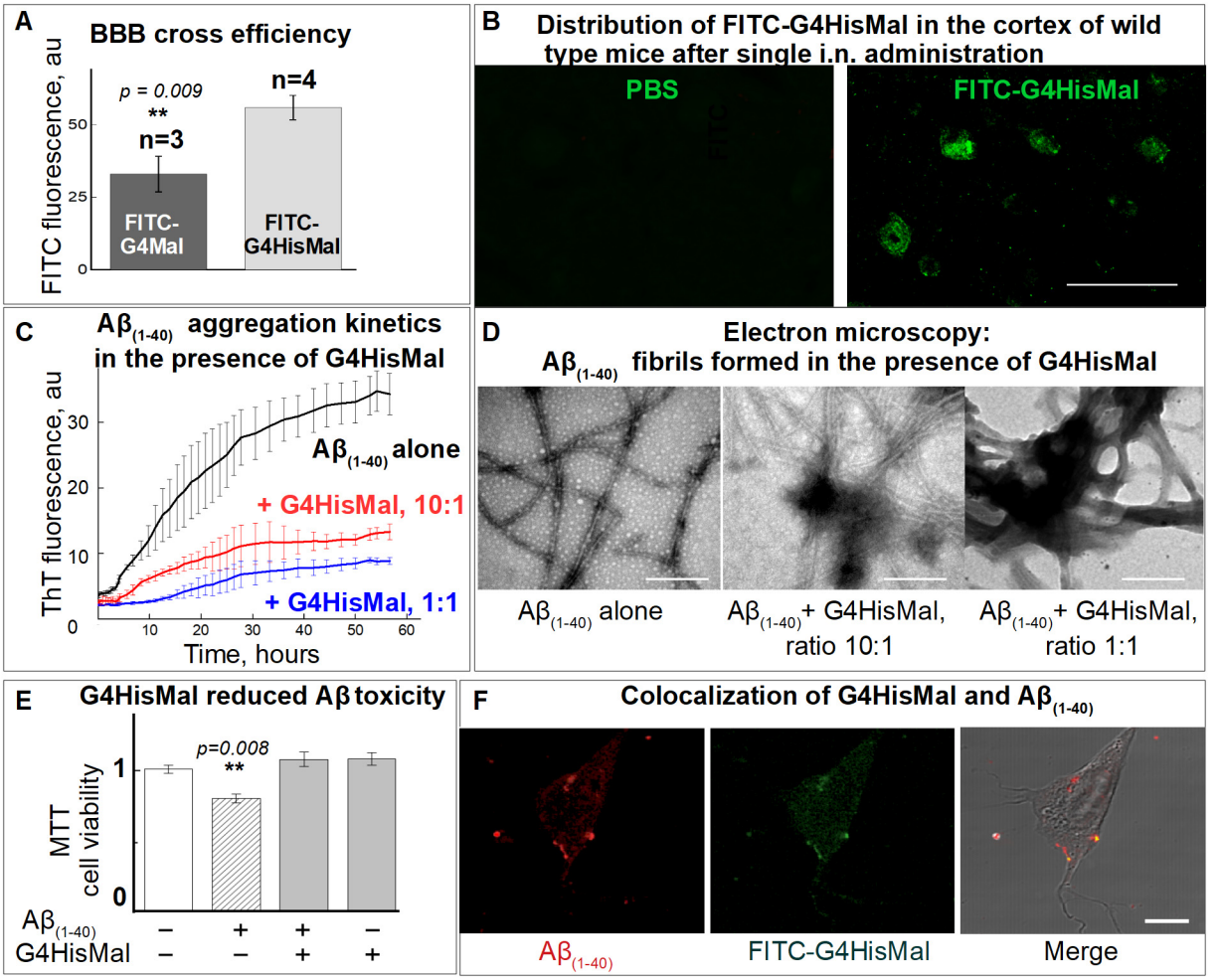

Figure 2. G4HisMal dendrimers cross the BBB and inhibit Aβ(1−40) induced cell toxicity. (**A**) FITC fluorescence of brain tissue homogenates after i.n. administration of FITC−G4HisMal and FITC−G4Mal. Statistics: Student's *t*-test, data are expressed as a mean ± SD; n = 3 per group. (**B**) Fluorescence microscopy images show the presence of FITC−G4HisMal in the cortex after i.n. administration of FITC−G4HisMal. The bar is 10 μm. (**C**) Aggregation of 20 μm $Aβ_{(1–40)}$ in the presence of G4HisMal. (**D**) Transmission electron microscopy (TEM): samples were collected at the end of ThT kinetics as shown in (C). Bar =100 nm. (**E**) MTT assay of $Aβ_{(1–40)}$ toxicity in the absence (dashed bar) and the presence of G4HisMal (gray bars). White columns correspond to control SH−SY5Y cells; these values are taken as 1 of cell viability. The experiment was repeated twice in triplicate. Statistics: one-way ANOVA followed by Tukey's post hoc test, data are expressed as a mean ± SD. (**F**) Colocalization of FITC-G4HisMal dendrimers with $Aβ_{(1–40)}$ in SH−SY5Y cells. SH−SY5Y cells were treated with 10 μmol $Aβ_{(1–40)}$ and 1 μmol G4HisMal after 24 hours of incubation, then cells were fixed and labeled with specific antibodies against $Aβ_{(1–40)}$ (red) 1 μmol and FITC against FITC-labeled dendrimers (green). Merge shows co-localization of $Aβ_{(1–40)}$ and FITC-G4HisMal. $Aβ_{(1–40)}$ fibrils and monomers were used as controls as shown in Figure S9. Scale bar is 20 μm.

intranasal (i.n.) administration was chosen as a noninvasive way of administration. To compare the ability to cross the BBB of G4HisMal with precursor G3Mal, dendrimers were conjugated with fluorescein isothiocyanate (FITC) as described.[18] FITC-G4HisMal and FITC-G3Mal dendrimers were administered intranasally to six-month-old wild-type mice at a dose of 10 mg/kg/(body weight). Animals treated with PBS were used as controls. One hour after treatment, animals were perfused with PBS, when blood was cleaned up from the brain blood vessels, the brains were removed FITC fluorescence in brain homogenate was measured. Our result demonstrate that FITC-G4HisMal has significantly improved ability to cross BBB compared to the precursor dendrimer, FITC-G3Mal. The efficiency of FITC-G3Mal to cross BBB is relatively low, as BBB penetration rate of G3Mal in brain tissue does not exceed 6 % of a single dose administered nasally to the mouse.[12] To evaluate BBB penetration rate of FITC-G4HisMal, we measured FITC fluorescence of brain homogenates prepared from animals treated with FITC conjugated G4HisMal, G4Mal and G3Mal. We documented that FITC fluorescence of G4HisMal was 40 % higher compared to maltose dendrimers, indicating that BBB penetration rate was 8.4 % from the total dose of 10 mg/kg/body weight used for intranasal administration. (Figure 2, *A*, Supplementary Figure 8). Importantly, we measured BBB cross of FITC-conjugated dendrimers, due to observed therapeutic effect of G4HisMal we suggest that non-conjugated G4HisMal may have higher BBB penetration rate. Of note, if brain perfusion were not sufficient to clean brain vessels from the

blood completely, then detected fluorescence might come from FITC-G4HisMal, which partially bypassed BBB. However, we believe that both type of dendrimers did cross BBB since transport of large molecular weight biologics into the brain along trigeminal and olfactory nerves as occurs within a minute.[24]

The presence of FITC-G4HisMal in brain tissue was confirmed by immunofluorescent labeling with an antibody specific to FITC (Figure 2, *B*). Thus, immunolabeling and direct measuring of FITC fluorescence demonstrated the presence of FITC-G4HisMal in the brain tissue after i.n. administration, indicating that FITC-G4HisMal dendrimers had crossed the BBB. Importantly, modification of G4Mal with histidine significantly improved the BBB cross 20 efficiency (Supplementary Figure 8). G4HisMal did not accumulate in the brain tissue after daily repeated i.n. administrations during one week and measured by FITC fluorescence in brain homogenate (data not shown).

Next, we tested G4HisMal capacity to interact with Alzheimer's amyloid peptides. As demonstrated by Thioflavin T (ThT) binding assay and electron transmission micrographs, G4HisMal dendrimers did not prevent fibril formation but clumped $A\beta_{(1-40)}$ fibrils together (Figure 2, *C, D*). Interestingly, the intensity of ThT was significantly decreased following the aggregation of $A\beta_{(1-40)}$. This observation can be explained that G4HisMal may compete with ThT for binding to $A\beta_{(1-40)}$ or G4HisMal may change $A\beta_{(1-40)}$ fibrillar resulting in lower ThT fluorescence quantum yield.[25,26] Similar results were obtained for aggregation kinetic of $A\beta_{(1-42)}$ (Supplementary Figure 9). Importantly, using electron microscopy, we did not detect any Aβ oligomers in the presence of G4HisMal. Our data demonstrated that G4HisMal significantly inhibit $A\beta_{(1-40)}$ cell toxicity for human neuroblastoma cells (Figure 2, *E*): The presence of 1 μmol G4HisMal, eliminated the toxicity of 10 μmol $A\beta_{(1-40)}$. Immunofluorescent labeling with a specific antibody against $A\beta_{(1\text{-}40)}$, showed co-localization of $A\beta_{(1-40)}$ and FITC-G4HisMal (Figure 2, *F*, Supplementary Figure 10). Interestingly, as detected by immunofluorescence, monomeric $A\beta_{(1-40)}$ was taken up by endocytic uptake,[27] while in the presence of G4HisMal, $A\beta_{(1-40)}$ was not taken up by the cells. Therefore, our data confirmed that when added to SHSY-5Y, G4HisMal did not affect cell viability itself and inhibited $A\beta_{(1-40)}$ induced cell toxicity.

Long-term G4HisMal treatment protects memory performance in APP-PS1 mice without reducing amyloid plaque load

To test anti-amyloid properties of G4HisMal in vivo, APP/PS1 mice were treated intranasally (i.n.) 5 μg/day of G4HisMal same volume of PBS was used as a control. G4HisMal treatment was started at the early pre-symptomatic stage when APP/Ps1 mice were 3 months of age and no memory impairment, nor amyloid plaques are normally detected.[19] Administration of G4HisMal was repeated three times per week and continued during three months until the APP/PS1 mice reached the age of 6 months when significant amyloid plaque load, synaptic loss, and memory dysfunction were manifested.[19] Age-matched wild-type mice were used as a control. Importantly, during the complete period of G4HisMal treatment, neither APP/PS1 nor wild-type mice did not demonstrate visible signs of weakness and apathy, indicating that the compound was well-tolerated. At the end of the treatment, after one week of drug wash-out period, all animals were exposed to the two-object recognition test. Strikingly, mice from APP/PS1 G4HisMal group demonstrated significant memory improvement when compared with the control mice, from APP/PS1-PBS group (Figure 3, *A*). Surprisingly, Aβ plaque quantification did not show a reduction in plaque load in the neocortex of treated APP/PS1 mice (Figure 3, *B*). However, we noticed distinct Aβ plaque morphology in the brain tissue of treated animals when compared to the Aβ plaques seen in the cortex of APP/PS1-PBS mice. To evaluate amyloid plaque morphology, total Aβ deposits were labeled with antibody 6E10; fibrillar Aβ was labeled with antibody OC.[28] Analysis of the plaque area as a ratio of the fibrillar Aβ (OC positive) against the total Aβ (6E10 positive) demonstrated a significant elevation of fibrillar content in amyloid plaques after G4HisMal treatment (Figure 3, *C*). Thus, G4HisMal modulated plaque morphology in vivo. Of note, we could not detect direct colocalization of amyloid plaque and G4HisMal in vivo, similar to our in vitro experiment, since for the treatment we used untagged G4HisMal.

Since inflammation and oxidative are strongly linked to AD,[29,30] we compared inflammation and oxidative stress markers in the brain tissue around the amyloid plaques between APP/PS1-G4HisMal and APP/PS1-PBS mice. Using GFAP and Iba1, as the markers of glial response, we did not observed significant differences around the amyloid plaques between G4HisMal treated and PBS groups (Figure 4, *A*). Using HNE and neuroketal as oxidative stress markers which have been shown to be increased in AD,[31,32] we did not detect significant differences in oxidative stress markers around amyloid plaques (Figure 4, *B*) nor in brain homogenate (Supplementary Figure 11). Taken together, results, shown in the Figures 3 and 4, indicated that more fibrillar amyloid plaques observed in G4HisMal group induced similar glial response and oxidative stress effects compared to less fibrillar plaques observed in the control PBS group. Therefore, we concluded that G4HisMal modulated morphology of amyloid plaques was not a direct cause of memory improvement after treatment.

Next, we quantified the levels and the ratio of soluble $A\beta_{42}$ to $A\beta_{40}$, using specific enzyme-linked immunosorbent assays (ELISA). Surprisingly, the ratio and levels of soluble $A\beta_{42}$ to $A\beta_{40}$ also were not changed after the G4HisMal treatment (Figure 5, *A*) indicating that as measured by ELISA, soluble Aβ were not related to the memory improvement of APP/PS1 mice. One possible explanation could be that for the memory loss in control APP/PS1-PBS animals were responsible soluble Aβ oligomers which could not be discriminated by ELISA. We hypothesized that G4HisMal could protect neurons form soluble Aβ oligomers. To test this hypothesis, we treated primary neurons derived from wild-type mouse embryos with 1μmol of freshly prepared of soluble $A\beta_{(1\text{-}42)}$ oligomers in the presence of G4HisMal. Using a release of lactate dehydrogenase (LDH) assay, we evaluated cell viability of cultured primary neurons in the presence of $A\beta_{(1\text{-}42)}$ and G4HisMal. As it was reviled by LDH assay, soluble $A\beta_{(1\text{-}42)}$ oligomers were the most toxic species for cultured neurons, whereas monomers and fibrils did

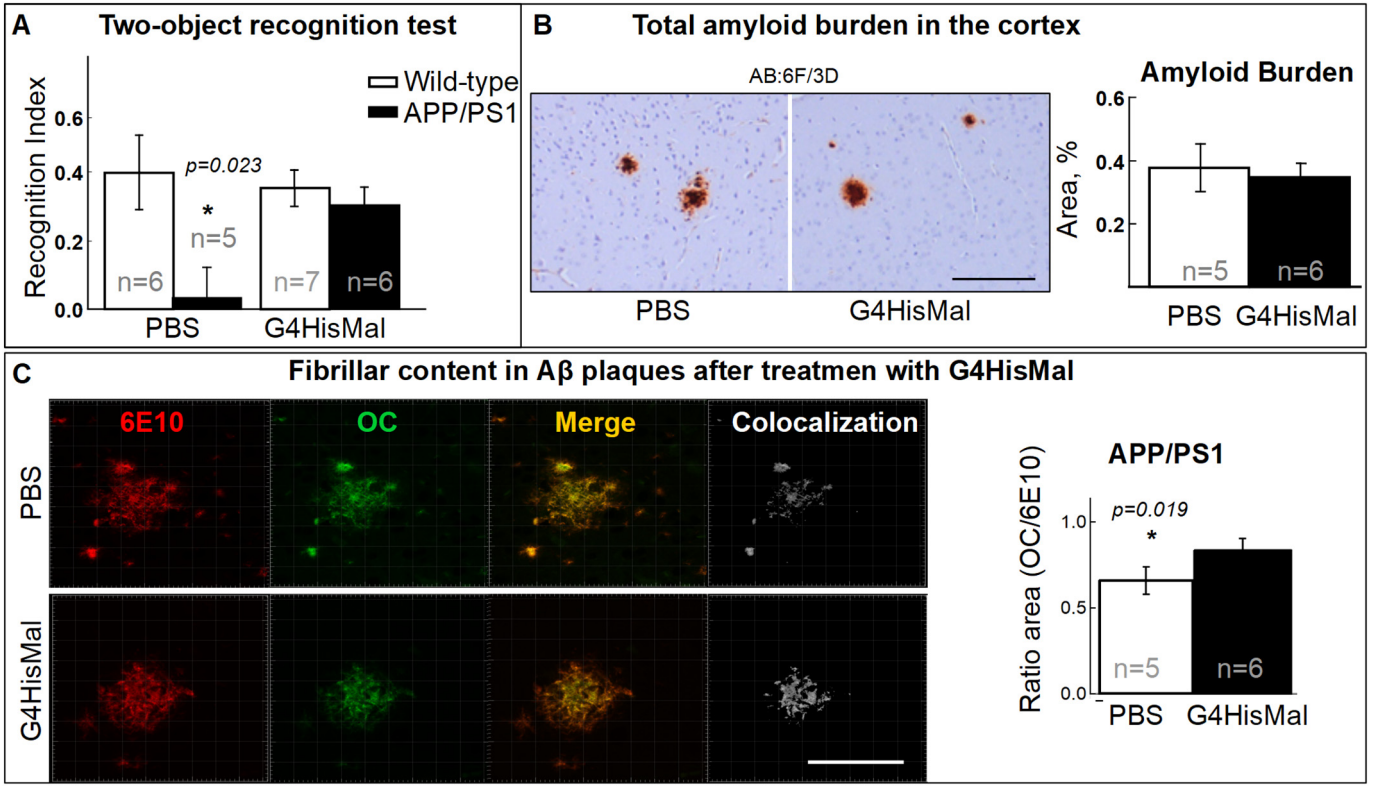

Figure 3. Long-term G4HisMal treatment protects memory performance in APP-PS1 mice and attenuates the morphology of amyloid plaques. (**A**) Memory performance in the V-maze shows significant improvement after treatment with G4HisMal. Statistics: two-way ANOVA with genotype and treatment as between factors followed by Tukey's post hoc test, data are expressed as a mean ± SEM. (**B**) Representative immunohistochemical images of 6F/3D-positive amyloid depositions. Scale bar is 100 μm. Statistics: one-way ANOVA followed by Tukey's post hoc test; data are expressed as a mean ± SEM. (**C**) Representative immunohistochemical images of OC and 6E10-positive amyloid depositions in the cortex. Scale bar is 50 μm. Statistics: Student's t-test; data are expressed as a mean ± SD.

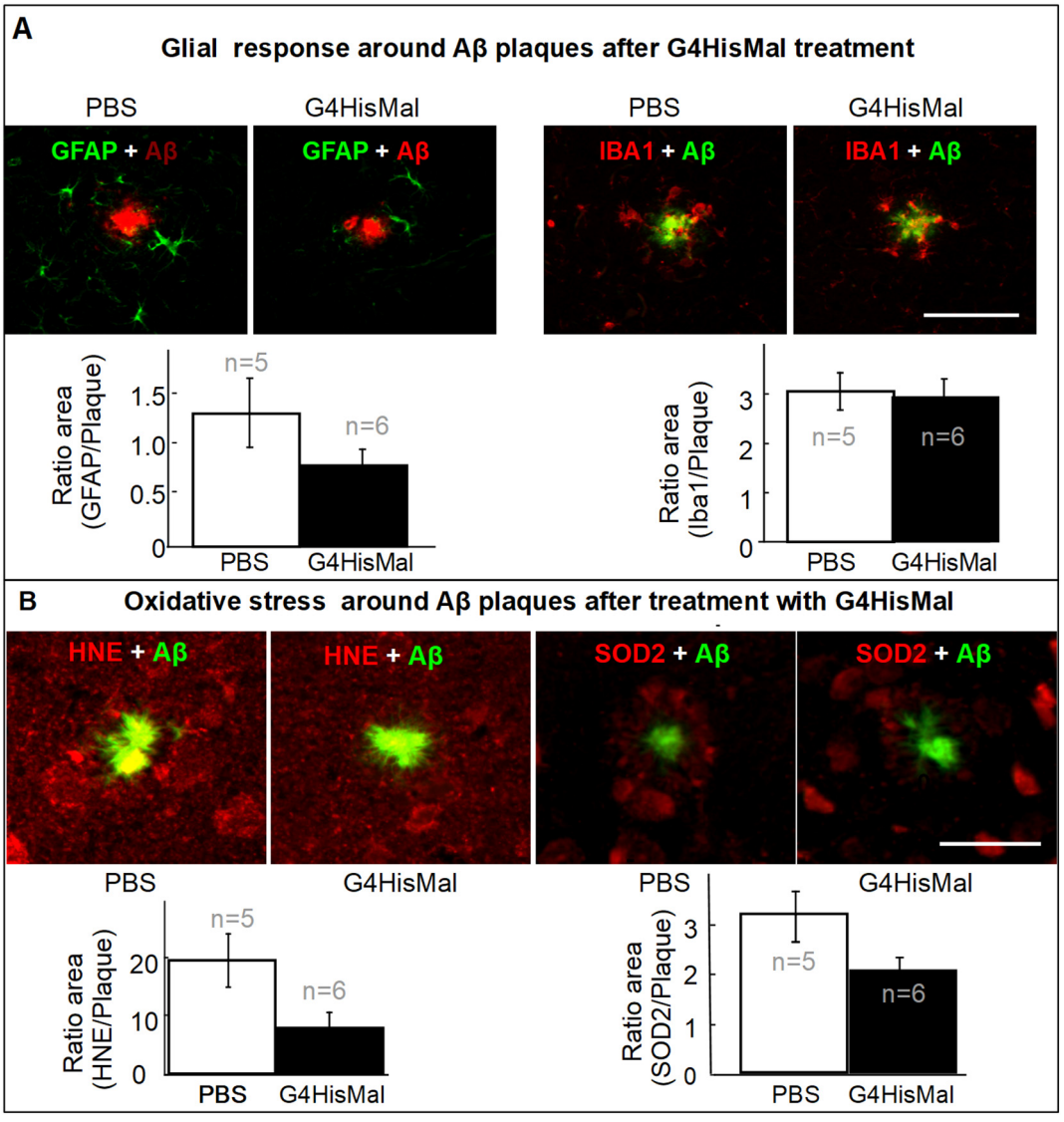

Figure 4. G4HisMal treatment does not modulate glial response and oxidative stress around Aβ plaques. (**A**) Glial response around amyloid plaques was not changed after G4HisMal treatment. Representative images of double immunofluorescence labeling of GFAP (green) and Aβ (red) (left panel) and Iba1 staining (red) and Aβ (green) (right panel) did not reveal a reduction of microglia and astrocytes around Aβ plaques after treatment. Scale bar is 50 μm. (**B**) Oxidative stress around amyloid plaques was not altered after G4HisMal treatment. Representative images of double immunofluorescence labeling of HNE (red) and Aβ (green) (left panel) and SOD2 staining (red) and Aβ (green) (right panel) did not detect a reduction of oxidative stress around Aβ plaques after treatment. Scale bar is 50 μm. Statistics: one-way ANOVA followed by Tukey's post hoc test; data are expressed as mean ± SEM.

not reduce cell viability during the incubation period. G4HisMal significantly reduced the neurotoxicity of soluble Aβ oligomers (Figure 5, *B*). Therefore, we conclude that G4HisMal was able to interfere with soluble neurotoxic $A\beta_{(1\text{-}42)}$ fraction reducing the neurotoxicity of soluble $A\beta_{(1\text{-}42)}$ oligomers.

Preventive G4HisMal treatment protects synapses

To understand a possible mechanism behind the memory rescue documented after G4HisMal treatment, we evaluated the level of pre- and postsynaptic markers using specific antibodies against drebrin, Pds95, and synaptophysin. All those synaptic markers play a role in the synaptic plasticity and are down-regulated in AD.[33,34] Western blotting with specific antibodies against synaptic markers demonstrated that synaptophysin, Psd95, and drebrin were up-regulated in brain homogenate of APP/PS1 mice treated with G4HisMal, compared to the controls, mice treated with PBS (Figure 6). Importantly, wild-type animals treated with G4HisMal did not show a difference in the level of synaptic markers as compared to wild-type PBS group (Supplementary Figure 11). Thus, G4HisMal treatment protected synapses in AD transgenic mice and was safe for wild-type mice. To study one of the possible mechanisms of synapse protection, we assayed the soluble fraction of brain homogenate using dot blot with specific oxidative stress markers. Taken together, our data demonstrated that first, G4HisMal protected synapses in the

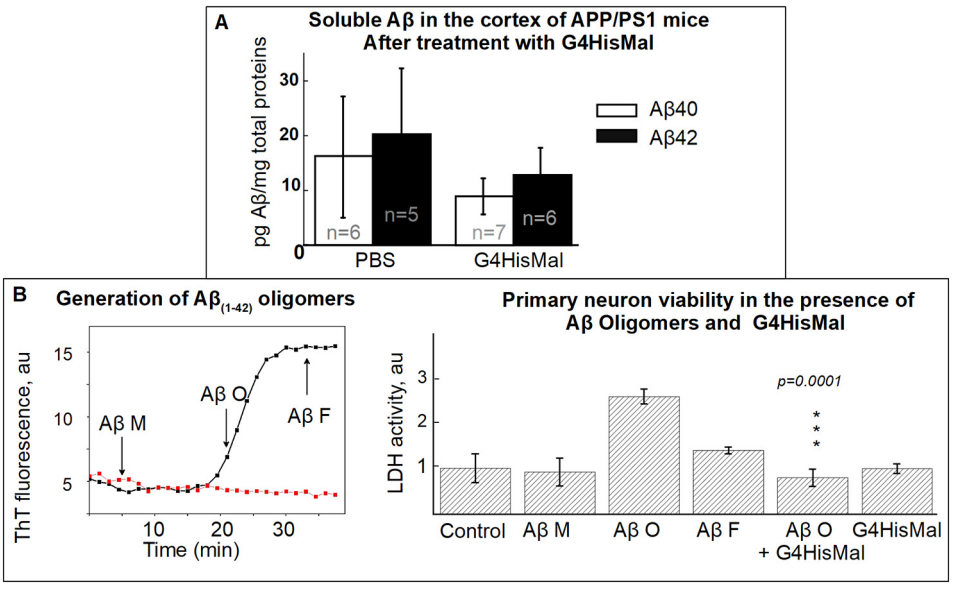

Figure 5. G4HisMal reduces the toxicity of Aβ oligomers for cultured primary neurons. (**A**) Soluble Aβ quantification: Enzyme-linked immunosorbent assay (ELISA), demonstrated that soluble Aβ was not changed in the brain extract of APP/PS1 G4HisMal mice. Statistics: one-way ANOVA followed by Tukey's post hoc test; data are expressed as mean ± SEM; n = 5 - 7 per group. (**B**) Left panel: Recombinant 10 μmol $Aβ_{(1–42)}$ was incubated at in PBS at 37°C. ThT fluorescence variation was used to monitor aggregation of $Aβ_{(1–42)}$ (black line), red line corresponds to ThT alone. The arrows indicate the time when aliquots of $Aβ_{(1–42)}$ monomers (Aβ M), oligomers (Aβ O), and fibrils (Aβ F) suspensions were taken for neuronal viability assay. Right panel: Wild-type primary neurons were treated for one hour with 1 μmol $Aβ_{(1–42)}$ monomers (Aβ M), oligomers (Aβ O), and fibrils (Aβ F), G4HisMal significantly reduces cytotoxicity of Aβ O. Statistics: one-way ANOVA followed by Tukey's post hoc test, data are expressed as a mean ± SD, n = 3 embryos per group.

brains of the treated APP-PS1mice; second, synapse protection in presymptomatic phase of AD could be an avenue for AD treatment and third, G4HisMal is a potential drug candidate for, synapse protection in presymptomatic phase of AD.

Discussion

Alzheimer's disease is a fatal neurodegenerative disorder and the most common cause of dementia in the elderly. Genetics strongly supports the hypothesis that aggregated Aβ is one of the players triggering degradation of synapses.[5,6] AD presymptomatic phase may last a decade or even more, and it is during this early phase, before the irreversible changes occur, therapies are most likely to be effective. In this study, we tested if preventive treatment with G4HisMal can protect APP/PS1 mice from memory impairment. Previously, maltose modified PPI dendrimers (G3Mal and G4Mal) have been suggested as promising modulators for the formation of the amyloid fibrillar structures related to certain proteinopathies diseases such as AD and prion diseases.[12,35] The interaction of G3Mal and G4Mal dendrimers with amyloid peptides is mainly tailored by hydrogen bonds depending on the density of hydrogen bond-forming sugar groups on the dendrimer surface.[36] However, being able to cross BBB and to interfere with Aβ, G3Mal does not improve clinical symptoms in vivo.[12] Therefore, we synthesized a novel type of dendrimers: 4th generation of PPI dendrimers with maltose-histidine shell, G4HisMal. In this study, we explored in vitro and in vivo the effects of G4HisMal. Our first objective was to assess whether histidine on the dendrimer shell can improve the biocompatibility and the ability to cross BBB of the precursor dendrimer G3Mal. The second objective was to investigate the potential of G4HisMal to protect AD transgenic mice from memory impairment. In vivo evaluations demonstrated that histidine maltose shell significantly improved biocompatibility and ability to cross BBB of PPI dendrimers; G4HisMal were able to interfere with Aβ fibril formation in vitro and in vivo; finally, chronic treatment with G4HisMal protected APP/PS1 mice from memory impairment. Since synaptic markers such as Psd95, synaptophysin, and drebrin were preserved after the G4HisMal treatment in AD transgenic mice, we suggest that the mechanism behind memory protection could be synapse shielding from soluble Aβ neurotoxicity.

The loss of synaptophysin immunoreactivity is the best-known correlate of cognitive decline in human AD[2] and, in AD transgenic models, synaptic markers such as synaptophysin and Psd-95 are also shown to be reduced.[34] Moreover, Psd95 knockout animals have learning defects and impaired basal synaptic transmission[37]; transgenic animals lacking synaptophysin have increased exploratory behavior and reduced novel object recognition.[38]

Interestingly, it has been shown that loss of synaptophysin immunoreactivity clearly preceded plaque formation, raising the possibility that Aβ can induce structural and functional neuronal deficits independent of plaque formation. Therefore, a treatment which may protect synapses is one of the avenues to fight against memory decline during AD.[3,39]

Here, three months of treatment with G4HisMal was able to prevent a decrease in synaptophysin and Psd95 synaptic markers compared to PBS-treated APP/PS1 mice. G4HisMal did not

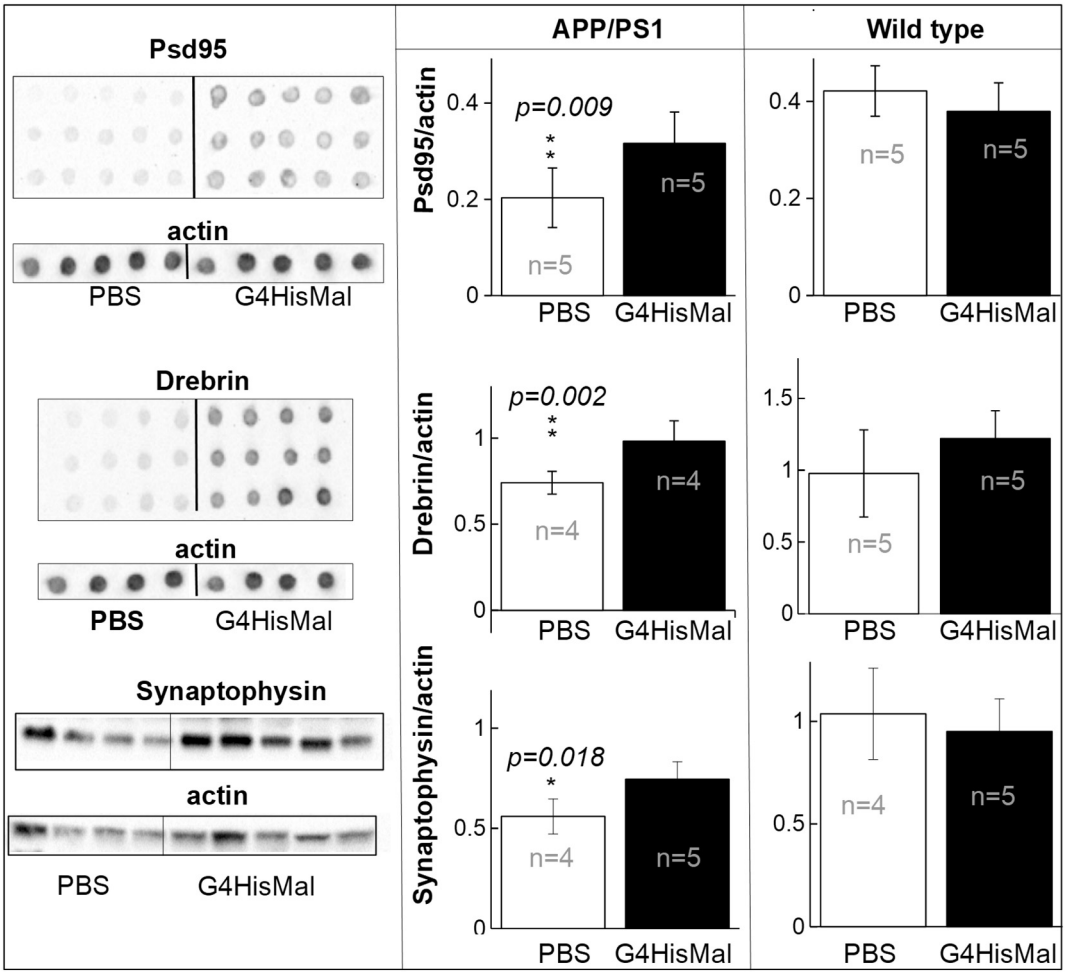

Figure 6. G4HisMal treatment protects synapses in APP/PS1 mice. Representative dot and Western blots of Psd95, drebrin, and synaptophysin. β-actin was used for protein normalization Statistics: Student's t-test. (n = 4-6 animals per group, dot and western blotting was done in triplicate). Data are expressed as a mean ± SD. Dot Blots and Western blots of Psd95, drebrin, synaptophysin for wild-type animals are shown in the Supplementary Figure 12.

change the level of Psd95, Synaptophysin, Drebrin in wild-type mice indicating that most likely the levels of mRNA expression of synaptic markers were not changed. Therefore, the increased levels of Psd95, Synaptophysin, Drebrin in treated APP/PS1 mice compared to the control group are more likely an effect of reduced degradation of synapses. Importantly, our results were reproducible, in two independent experiments we got similar results demonstrating memory protection after G4HisMal treatment.

However, since the analysis of mRNA expression of synaptic markers was not possible in this study due to brain homogenate preparation, future experiments are required to determine thoroughly what mechanism(s) is/are behind the protection of synapses by G4HisMal. Also, the interaction of G4HisMal with soluble Aβ pool should be further assessed in vivo including the response of neurons, astrocytes, and microglia.

To conclude, we demonstrated that histidine-maltose shell significantly improves biocompatibility of PPI dendrimers and their ability to cross BBB. Therefore, we suggest that maltose-histidine shell may be used to improve biocompatibility and ability to cross BBB of other types of dendrimers. We proved that during chronic administration (during three months) of G4HisMal was able to cross BBB and G4HisMal treatment rescued spatial memory deficits in APP/PS1 mice possibly via shielding of synapses against soluble Aβ oligomers. Thus, G4HisMal is an effective and safe agent suitable for treatment of the central nervous system.

Acknowledgments

We thank the Saxon Ministry of Science and Art (SMWK), the German Federal Ministry for Education and Science (BMBF), COST-Action program TD0802 (Biodendrimers in biomedical applications), Swedish Research Council 2017-01539 and MultiPark (Medical Faculty, Lund University).

Appendix A. Supplementary data

Supplementary data to this article can be found online at https://doi.org/10.1016/j.nano.2019.01.010.

References

1. Ferrer I. Defining Alzheimer as a common age-related neurodegenerative process not inevitably leading to dementia. *Prog Neurobiol* 2012;**97**:38-51.
2. Terry RD, Masliah E, Salmon DP, Butters N, DeTeresa R, Hill R, et al. Physical basis of cognitive alterations in Alzheimer's disease: Synapse loss is the major correlate of cognitive impairment. *Ann Neurol* 1991;**30**:572-80.
3. Mucke L, Masliah E, Yu GQ, Mallory M, Rockenstein EM, Tatsuno G, et al. High-level neuronal expression of abeta 1-42 in wild-type human amyloid protein precursor transgenic mice: synaptotoxicity without plaque formation. *J Neurosci* 2000;**20**:4050-8.
4. Masliah E. Recent advances in the understanding of the role of synaptic proteins in Alzheimer's Disease and other neurodegenerative disorders. *J Alzheimers Dis* 2001;**3**:121-9.
5. Tu S, Okamoto S, Lipton SA, Xu H. Oligomeric Aβ-induced synaptic dysfunction in Alzheimer's disease. *Mol Neurodegener* 2014;**9**:48.
6. Klementieva O, Willén K, Martinsson I, Israelsson B, Engdahl A, Cladera J, et al. Pre-plaque conformational changes in Alzheimer's disease-linked Aβ and APP. *Nat Commun* 2017;**8**:14726.
7. Madaan K, Poonia N, Kumar S, Lather V. Dendrimers in drug delivery and targeting: Drug-dendrimer interactions and toxicity issues. *J Pharm Bioallied Sci* 2014;**6**:139.
8. Svenson S, Tomalia DA. Dendrimers in biomedical applications—reflections on the field. *Adv Drug Deliv Rev* 2012;**64**:102-15.
9. Kannan RM, Nance E, Kannan S, Tomalia DA. Emerging concepts in dendrimer-based nanomedicine: from design principles to clinical applications. *J Intern Med* 2014;**276**:579-617.
10. Huang R-Q, Qu Y-H, Ke W-L, Zhu J-H, Pei Y-Y, Jiang C. Efficient gene delivery targeted to the brain using a transferrin-conjugated polyethyleneglycol-modified polyamidoamine dendrimer. *FASEB J* 2007;**21**:1117-25.
11. Sharma R, Kim S-Y, Sharma A, Zhang Z, Kambhampati SP, Kannan S, et al. Activated microglia targeting dendrimer–minocycline conjugate as therapeutics for neuroinflammation. *Bioconjug Chem* 2017;**28**:2874-86.
12. Klementieva O, Aso E, Filippini D, Benseny-Cases N, Carmona M, Juvés S, et al. Effect of poly(propylene imine) glycodendrimers on β-amyloid aggregation in vitro and in APP/PS1 transgenic mice, as a model of brain amyloid deposition and Alzheimer's disease. *Biomacromolecules* 2013;**14**:3570-80.
13. Yamakami J, Sakurai E, Sakurada T, Maeda K, Hikichi N. Stereoselective blood-brain barrier transport of histidine in rats. *Brain Res* 1998;**812**:105-12.
14. Oshima T, Oshima C, Baba Y. Selective extraction of histidine derivatives by metal affinity with a copper(II)–chelating ligand complex in an aqueous two-phase system. *J Chromatogr B* 2015;**990**:73-9.
15. Wang H, Wang M, Wang B, Li M, Chen H, Yu X, et al. The distribution profile and oxidation states of biometals in APP transgenic mouse brain: dyshomeostasis with age and as a function of the development of Alzheimer's disease. *Metallomics* 2012;**4**:289.
16. Tang S-C, Arumugam TV, Cutler RG, Jo D-G, Magnus T, Chan SL, et al. Neuroprotective actions of a histidine analogue in models of ischemic stroke: Histidine analogue in models of ischemic stroke. *J Neurochem* 2007;**101**:729-36.
17. Mark JE, editor. *Polymer data handbook*. 2nd ed. Oxford; New York: Oxford University Press; 2009.
18. Janaszewska A, Ziemba B, Ciepluch K, Appelhans D, Voit B, Klajnert B, et al. The biodistribution of maltotriose modified poly(propylene imine) (PPI) dendrimers conjugated with fluorescein—proofs of crossing blood–brain–barrier. *New J Chem* 2012;**36**:350-3.
19. Aso E, Lomoio S, López-González I, Joda L, Carmona M, Fernández-Yagüe N, et al. Amyloid generation and dysfunctional immunoproteasome activation with disease progression in animal model of familial Alzheimer's disease: amyloid generation and UPS in FAD mice. *Brain Pathol* 2012;**22**:636-53.
20. Willén K, Edgar JR, Hasegawa T, Tanaka N, Futter CE, Gouras GK. Aβ accumulation causes MVB enlargement and is modelled by dominant negative VPS4A. *Mol Neurodegener* 2017;**12**, https://doi.org/10.1186/s13024-017-0203-y.
21. Boas U, Heegaard PMH. Dendrimers in drug research. *Chem Soc Rev* 2004;**33**:43.
22. Fischer M, Appelhans D, Schwarz S, Klajnert B, Bryszewska M, Voit B, et al. Influence of surface functionality of poly(propylene imine) dendrimers on protease resistance and propagation of the scrapie prion protein. *Biomacromolecules* 2010;**11**:1314-25.
23. Liu Q, Shen Y, Chen J, Gao X, Feng C, Wang L, et al. Nose-to-brain transport pathways of wheat germ agglutinin conjugated PEG-PLA nanoparticles. *Pharm Res* 2012;**29**:546-58.
24. Lochhead JJ, Thorne RG. Intranasal delivery of biologics to the central nervous system. *Adv Drug Deliv Rev* 2012;**64**:614-28.
25. Jimenez JL, Nettleton EJ, Bouchard M, Robinson CV, Dobson CM, Saibil HR. The protofilament structure of insulin amyloid fibrils. *Proc Natl Acad Sci* 2002;**99**:9196-201.
26. Sulatskaya AI, Kuznetsova IM, Turoverov KK. Interaction of Thioflavin T with amyloid fibrils: fluorescence quantum yield of bound dye. *J Phys Chem B* 2012;**116**:2538-44.
27. Wesén E, Jeffries GDM, Matson Dzebo M, Esbjörner EK. Endocytic uptake of monomeric amyloid-β peptides is clathrin- and dynamin-independent and results in selective accumulation of Aβ(1–42) compared to Aβ(1–40). *Sci Rep* 2017;**7**, https://doi.org/10.1038/s41598-017-02227-9.
28. Kayed R, Head E, Sarsoza F, Saing T, Cotman CW, Necula M, et al. Fibril specific, conformation dependent antibodies recognize a generic epitope common to amyloid fibrils and fibrillar oligomers that is absent in prefibrillar oligomers. *Mol Neurodegener* 2007;**2**:18.
29. Birch AM, Katsouri L, Sastre M. Modulation of inflammation in transgenic models of Alzheimer's disease. *J Neuroinflammation* 2014;**11**:25.
30. Cheignon C, Tomas M, Bonnefont-Rousselot D, Faller P, Hureau C, Collin F. Oxidative stress and the amyloid beta peptide in Alzheimer's disease. *Redox Biol* 2018;**14**:450-64.
31. Dalleau S, Baradat M, Guéraud F, Huc L. Cell death and diseases related to oxidative stress:4-hydroxynonenal (HNE) in the balance. *Cell Death Differ* 2013;**20**:1615-30.
32. Gonzalo H, Brieva L, Tatzber F, Jové M, Cacabelos D, Cassanyé A, et al. Lipidome analysis in multiple sclerosis reveals protein lipoxidative damage as a potential pathogenic mechanism. *J Neurochem* 2012;**123**:622-34.
33. Shim KS, Lubec G. Drebrin, a dendritic spine protein, is manifold decreased in brains of patients with Alzheimer's disease and Down syndrome. *Neurosci Lett* 2002;**324**:209-12.
34. Poirel O, Mella S, Videau C, Ramet L, Davoli MA, Herzog E, et al. Moderate decline in select synaptic markers in the prefrontal cortex (BA9) of patients with Alzheimer's disease at various cognitive stages. *Sci Rep* 2018;**8**, https://doi.org/10.1038/s41598-018-19154-y.
35. McCarthy JM, Franke M, Resenberger UK, Waldron S, Simpson JC, Tatzelt J, et al. Anti-Prion drug mPPIg5 inhibits PrPC conversion to PrPSc. *PLoS One* 2013;**8**e55282.
36. Klementieva O, Benseny-Cases N, Gella A, Appelhans D, Voit B, Cladera J. Dense shell glycodendrimers as potential montoxic anti-amyloidogenic agents in Alzheimer's disease. Amyloid–dendrimer aggregates morphology and cell toxicity. *Biomacromolecules* 2011;**12**:3903-9.
37. Nagura H, Ishikawa Y, Kobayashi K, Takao K, Tanaka T, Nishikawa K, et al. Impaired synaptic clustering of postsynaptic density proteins and altered signal transmission in hippocampal neurons, and disrupted learning behavior in PDZ1 and PDZ2 ligand binding-deficient PSD-95 knockin mice. *Mol Brain* 2012;**5**:43.

38. Schmitt U, Tanimoto N, Seeliger M, Schaeffel F, Leube RE. Detection of behavioral alterations and learning deficits in mice lacking synaptophysin. *Neuroscience* 2009;**162**:234-43.
39. Tampellini D, Capetillo-Zarate E, Dumont M, Huang Z, Yu F, Lin MT, et al. Effects of synaptic modulation on amyloid, synaptophysin, and memory performance in Alzheimer's disease transgenic mice. *J Neurosci* 2010;**30**:14299-304.
40. Petoukhov MV, Franke D, Shkumatov AV, Tria G, Kikhney AG, Gajda M, et al. New developments in the *ATSAS* program package for small-angle scattering data analysis. *J Appl Crystallogr* 2012;**45**:342-50.
41. Pettersen EF, Goddard TD, Huang CC, Couch GS, Greenblatt DM, Meng EC, et al. UCSF Chimera? A visualization system for exploratory research and analysis. *J Comput Chem* 2004;**25**:1605-12.